International Journal of Recent Technology and Engineering (IJRTE)
ISSN: 2277-3878, Volume-8 Issue-5, January 2020

Implementation of MOIDS Algorithm for Optimal Parameter Selection of SFPT for Modern Radars

K. Ravi Kumar, P. Rajesh Kumar, Satish Kumar Injeti

Abstract: ***Modern radars require signals of the large frequency range to attain relatively greater range resolution. Frequency stepping is the technique to convert the narrowband signal, i.e., a train of pulses into a wideband signal to achieve high accuracy in range resolution measurements. Due to the cause of constant step in frequency of successive pulses, grating lobes appeared when the period of pulse multiplied by step in frequency exceeds unity as is needed in modern radars. Hence to achieve the best resolution, grating lobes height, sidelobes level, and mainlobe width have to be minimum. In this paper an attempt has been made to diminish grating lobes, minimize sidelobes and reduce mainlobe width using MOIDSA to find the parameters of Stepped Frequency Pulse Train (SFPT) mechanism. The compromise between various lobes is obtained by using three dimensional Pareto fronts for different ranges of SFPT parameters.***

Index Terms: ***Stepped frequency pulse train, Autocorrelation function, Grating lobes, Sidelobes, Mainlobe width and Multi-optimization algorithms.***

I. INTRODUCTION

In any radar system most commonly used radar signals are the frequency modulated and phase modulated signals [1]. The selection of an appropriate signal depends on the particular field of use. It is necessary to design for optimum detection. Ideally, the waveform must provide minimum lack of clarity when the signal is reflected to determine the desired data regarding range quantity of true targets and velocity. Pulse compression [2, 3] has emerged as an important processing operation. The resolution of the range is a function of pulse width [4]. By increasing the pulse length, peak power can be reduced. But, an increase in the length of the pulse reduces range resolution [5]. A compromise is achieved by some form of encoding, which must be carried out during transmission. So that a longer pulse can be compressed into a shorter one in the receiver using the technique of signal processing

Manuscript received on January 02, 2020.
Revised Manuscript received on January 15, 2020.
Manuscript published on January 30, 2020.

* Correspondence Author

Dr. K. Ravi Kumar, Department of ECE, N. S. Raju Institute of Technology, Sontyam, Visakhapatnam, Andhra Pradesh 530003, India.

Prof. P. Rajesh Kumar, Department of ECE, A U College of Engineering (A), Andhra University, Visakhapatnam, Andhra Pradesh 530003, India.

Dr. Satish Kumar Injeti, Department of Electrical Engineering, National Institute of Technology, Warangal, Telengana State 506004, India.

For wideband operations, LFM signals [6] are suitable. Stepped frequency pulse train shown in Figure 1 is used to support the narrowband hardware system to achieve high range resolution [7].

Due to the constant step between the pulses, the unwanted spikes known as grating lobes are presented in the Autocorrelation function at every period of $1/\Delta f$. Due to the cause of grating lobes, the range resolution will be decreased. In [8, 9], authors propose various techniques to diminish the grating lobes without considering the sidelobes and mainlobe width. The false alarm can occur due to sidelobes, and range resolution is decreased if mainlobe width is increased. The author in [10] applied spectral weighting, in this method the sensitivity of the signal will be decreased. To diminish the grating lobes, a non-linear frequency modulated (NLFM) signal is introduced in the stepped pulse train. But NLFM signal is not Doppler tolerant one [11]. To overcome these problems, the author in [12] proposes a Non-dominated sorting genetic algorithm (NSGA-II) [13] to obtain proper parameters of SFPT signal to diminish grating lobes, minimize the sidelobes and reduce mainlobe width. The computation time in NSGA-II is more because of its complexity $O(MN)^2$. To overcome the difficulties, authors in [14] proposed Multi-objective Grasshopper optimization algorithm (MOGOA) to determine optimum values to get a number of non-dominated solutions with fast convergence using two dimensional Pareto fronts. In this paper Multi-objective improved differential search algorithm (MOIDSA) is applied to set the optimized parameters [15-17] of SFPT for diminishing the grating lobes, reducing the mainlobe width and decreasing sidelobes to achieve high range resolution. The compromise of mainlobe width, grating lobe amplitude, and sidelobe level are obtained using three dimensional Pareto fronts.

The remaining portion is organized as: section II, gives the Analysis of SFPT signal. Section III deals the problem formulation of MOIDSA. Overview of MOIDSA is presented in section IV. Simulation results of MOIDSA are discussed in section V. Finally, section VI gives the Concluding remarks.

II. ANALYSIS OF SFPT

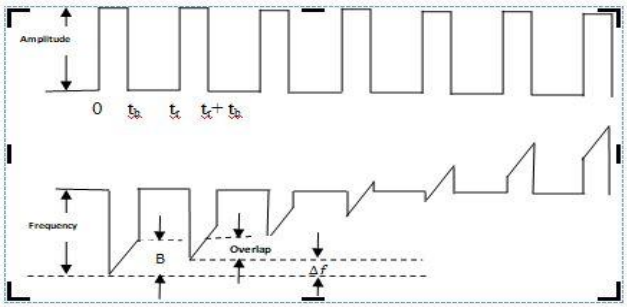

Figure 1: Stepped Frequency Pulse Train

The complex shape of pulse without modulation (duration t_b) is given by

$$u(t) = \frac{1}{\sqrt{t_b}} rect\left(\frac{t}{t_b}\right)$$

(1)

The unmodulated pulse is modulated by LFM wave form to increase the bandwidth, is given as

$$u_1(t) = \frac{1}{\sqrt{t_b}} rect\left(\frac{t}{t_b}\right) exp(j\pi kt^2)$$

(2)

k denotes frequency slope and is given by

$$k = \pm \frac{B_1}{t_b}$$

Signs are for frequency slope + ve and – ve value of k is valid.

The ACF of u_s(t) is given [10] as

$$|R(\tau)| = \left|\left(1-\frac{|\tau|}{t_b}\right) sinc\left[B\tau\left(1-\frac{|\tau|}{t_b}\right)\right]\right| \left|\frac{sin(N\pi\tau\,\Delta f)}{N\,sin(\pi\tau\,\Delta f)}\right|$$

(3)

The expression for $|R(\tau)|$ is basically a product of two items. First one is the ACF of LFM pulse is represented as

$$|R_1(\tau)| = \left|\left(1-\frac{|\tau|}{t_b}\right) \sin c\left[B\tau\left(1-\frac{|\tau|}{t_b}\right)\right]\right|$$

(4)

The second often term gives grating lobes.

$$|R_2(\tau)| = \left|\frac{\sin(N\pi\tau\,\Delta f)}{N\sin(\pi\tau\,\Delta f)}\right|$$

(5)

III. PROBLEM FORMULATION

The aim of problem formulation is (a) minimize side lobes and reduce grating lobes to get small echoes response and (b) decreasing the mainlobe width to improve range resolution. The problem is formulated for getting the trade-off solution between grating lobes, sidelobes and main lobe width.

The performance evaluation is done by obtaining peak to sidelobe level ratio (PSLR) [18]

$$PSLR(dB) = 20\log_{10}\frac{\max_{1\le l\le N}|R(l)|}{|R(0)|}$$

(6)

R (0) is the mainlobe level, and $R(l)$ is maximum sidelobe level among all sidelobes.

$|R_1(\tau)|$ *and* $|R_2(\tau)|$ are the functions of $t_b\Delta f$ *and* $t_b B$. $N\Delta f$ should always be greater than B to get a meaningful increase in bandwidth. The value of $t_b B$ is chosen such that $t_b B = (c+1)t_b\Delta f$ to ensure $B > \Delta f$.

MOIDSA approach

The authors [12, 14] propose the Multi-Objective Optimization (MOO) approach for problem formulation to get the balance among various lobes In this paper, MOIDSA is used to achieve the optimized parameters to diminish grating lobes, minimize sidelobes to avoid false alarm and reduce mainlobe width to achieve high resolution in range with the help of three dimensional Pareto fronts.

The objective functions to be optimized given as

$$\begin{cases} \text{Minimize} \quad f_1 = \max\,[\,|R_1(\tau_g)|] \text{ where } g = 1, 2, \ldots, \lfloor t_b\Delta f \rfloor \\ \text{Minimize} \quad f_2 = \text{PSLR in dB} \\ \text{Minimize} \quad f_3 = \dfrac{1}{N\,t_b\Delta f} \end{cases}$$

(7)

Subjected to the constraints

$N\,t_b\Delta f > t_b\,B$ *and* $[\,|R_1(\tau_g)|] < \varepsilon$

Decreasing the width of mainlobe and the highest level of sidelobe by setting the grating lobes at some threshold level (ε). The minimum of $|R_2(\tau)|$ corresponds to $1/Nt_b\Delta f$, whereas that of $|R_1(\tau)|$ corresponds nearly if $1/t_b B >> 1$. So, the first null of ACF is given by

$$\frac{\tau_{1st\quad null}}{t_b} = \min\left(\frac{1}{t_b B}, \frac{1}{Nt_b\Delta f}\right)$$

(8)

IV. MOIDS ALGORITHM

The improved differential search algorithm is the latest version of Differential Search Algorithm (DSA) developed by Civicioglu in the year 2013 [19]. DSA is based on the migration of living beings for food during variations of climate. The multi-objective format of IDSA [20 and 21] named as MOIDSA [22] reduces minimum and increases a maximum of multiple objective functions.

$$Minimize\ F(x) = \{f_1(x), \ldots\ldots f_{N_{obj}}(x)\} \quad where\ N_{obj}\ is\ number\ of\ objectives$$

$$x = [X_1, X_2, \ldots\ldots X_d] \quad where\ d\ is\ number\ of\ variables$$

(9)

Instead of one solution, optimal solutions are obtained. It is difficult to evaluate all the solutions. So, no global optimum solutions can be fixed. Hence a group of Pareto optimal solutions comes up, such that these are not surpassed by any other solutions. Here a decision vector X_1 dominates a counter part X_2 iff X_1 is partially less.

$$\forall i \in \{1,2,.....N_{obj}\}: f_i(X_1) \le f_i(X_2)$$
$$\exists_j \in \{1,2,.....N_{obj}\}: f_j(X_1) \le f_j(X_2)$$

(10)

Implementation Strategy for MOIDS Algorithm

The optimal tuning of $t_b\Delta f$ and c is the bases of implementation.

Step 1: Initialization

Population size (NP), problem dimension (D) and a maximum number of generations (G_{max}) are initially assigned randomly. Limits of $t_b\Delta f$ and c also initialized.

Step 2: Organism population ($t_b\Delta f$ and c)

For getting organism population random generation is adapted

$$X = \begin{bmatrix} x_1^1 & x_2^1 & \cdots & x_{d-1}^1 & x_d^1 \\ x_1^2 & x_2^2 & \cdots & x_{d-1}^2 & x_d^2 \\ \vdots & \vdots & \vdots & \vdots & \vdots \\ x_1^{pop-1} & x_2^{pop-1} & \cdots & x_{d-1}^{pop-1} & x_d^{pop-1} \\ x_1^{pop} & x_2^{pop} & \cdots & x_{d-1}^{pop} & x_d^{pop} \end{bmatrix}$$

(11)

$$x_i^j = x_{\min,i} + (x_{\max,i} - x_{\min,i}) * rand()$$

(12)

Here,

(a) d gives the quantity of decision variables
(b) pop gives population.
(c) x_i^j is based on $t_b\Delta f$ and c
(d) rand() is a random number in between 0 and 1

$$[x_1^1 x_2^1 x_{d-1}^1 x_{d-1}^1] = [t_b\Delta f^1,\ c^1]$$

(13)

X represents the ensemble of living beings on artificial organisms which is one place in search space is given by a solution containing $t_b\Delta f$ and c values.

Step 3: Calculate fitness function value

Evaluate population X using Eq. 7.

Step 4: Locate non-dominated solutions.

Step 5: The Non-dominated solution is segregate and stored in the archive with $G = 0$.

Step 6: Initiate evolution procedure.

Step 7: Search process is performed, and stopover vector is generated using Eq. 14, Eq. 16 and Eq.17.

$$s_i = X_{r1} + scale.(X_{r2} - X_i)$$

(14)

$$scale = randg(2*rand)*(rand - rand)$$

(15)

$$s_{i,j,G}^t = \begin{cases} s_{i,j,G} & if \quad r_{i,j} = 0 \\ X_{i,j,G} & if \quad r_{i,j} = 1 \end{cases}$$

(16)

$$x_{i,G+1} = \begin{cases} s_{i,G} & if \quad f(s_{i,G}^t) \le f(x_{i,G}) \\ x_{i,G} & if \quad f(s_{i,G}^t) > f(x_{i,G}) \end{cases}$$

(17)

Step 8: Evaluate each member of stopover vector

Evaluate stopover vector according to objective functions using Eq. 7 for locating an individual member of stopover vector.

Step 9: Check for dominance stopover vector

Stopover vector stored ideally dominates the artificial organisms vector population. Discard stopover vector if artificial organism dominates. Else, it is added to the population (temp pop).

Step 10: Latest solution vector is added to temp pop

Crowding assignment and non dominated solution help in selecting next generation. Non dominated solutions are stored in the repository. When the capacity of the repository is high, the crowded members are selected by crowding assignment operators.

Step 11: Initiate stopping procedure

Generation counter is incremented and termination criteria checked. If the G has reached the maximum point, the non dominated solution is printed out, and the process is retarded. Else, step 6 and step 10 are repeated.

V. RESULTS AND DISCUSSION

Authors [12, 14] used two dimensional approaches to achieve the compromise between sidelobes to grating lobes and sidelobes versus mainlobe width separately. In this paper, three dimensional Pareto fronts are proposed to obtain the nearest optimized values of reduced mainlobe width, diminished grating lobe level and minimized peak sidelobe level at a time using MOIDSA.

Simulation results are carried out using MOIDSA for obtaining the optimum values of $t_b\Delta f$ and c in the range $t_b\Delta f \in [2, 10]$, $c \in [2, 10]$, $\varepsilon < 0.01$ and N = 8, $t_b\Delta f \in [2, 10]$, $c \in [2, 5]$, $\varepsilon = 0.01$ and N = 8 and $t_b\Delta f \in [5, 30]$, $c \in [2, 10]$, $\varepsilon < 0.01$ and N = 8. In all ranges mainlobe width is considered $\varepsilon = 0.045$. The population size and generations are taken to be 200 and 50.

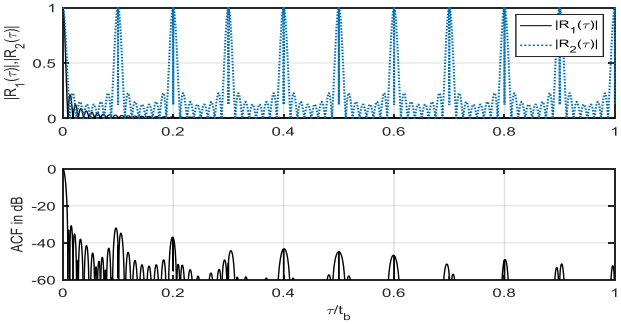

Figure 2: SFPT for $t_b\Delta f$ =10, c =10 and t_bB =110, N = 8. Top shows $|R_1(\tau)|$ (solid) and $|R_2(\tau)|$ (dash) where as bottom shows values of ACF (dB).

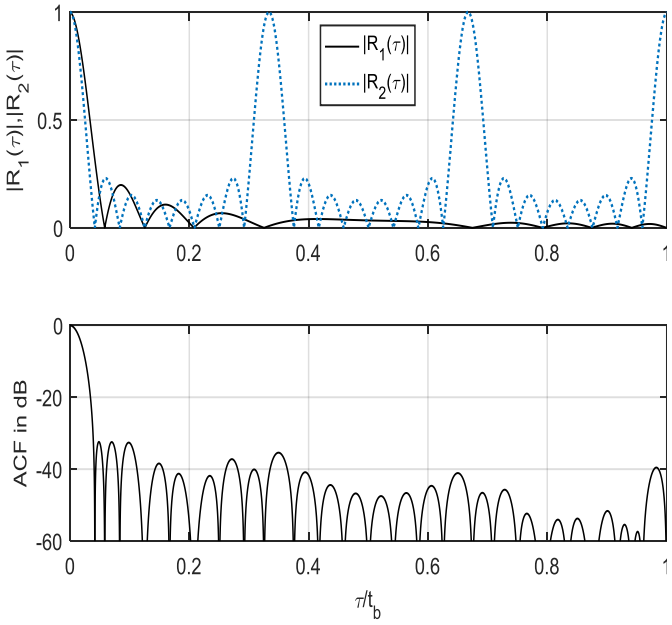

Figure 3: SFPT for $t_b\Delta f$ =2.9971, c =5.0801 and t_bB=18.223, N = 8. Top shows $|R_1(\tau)|$ and $|R_2(\tau)|$, bottom shows values of ACF (dB).

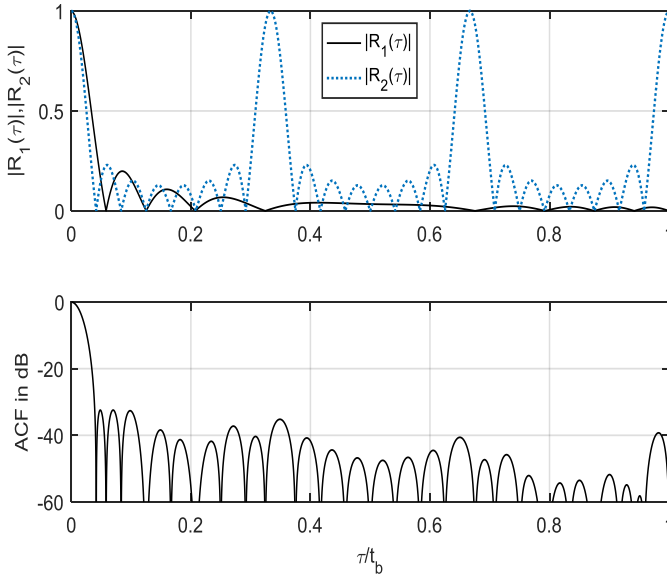

Figure 4: SFPT for $t_b\Delta f$ =2.9998, c =5.0830 and t_bB=18.248, N = 8. Top shows $|R_1(\tau)|$ and $|R_2(\tau)|$, bottom shows values of ACF (dB).

In the range $t_b\Delta f \in [2,10]$, $c \in [2,10]$ and N = 8, the Figure 2 shows the grating lobes are almost near to zero and PSLR is obtained -30.713 dB and mainlobe width is 0.0125. Figure 3 gives the PSLR of -32.412 dB when the grating lobe amplitude is 0.0076 and mainlobe width is 0.0417. In Figure 4, when the grating lobe amplitude is increased to 0.0086, PSLR is increased to -32.434 dB. From the evidence of Figure 2, Figure 3 and Figure 4, it can be concluded that, the PSLR is changed from -30.713 dB to -32.434 dB with the changes of Parameters of the SFPT. The corresponding Pareto front is shown in Figure 5.

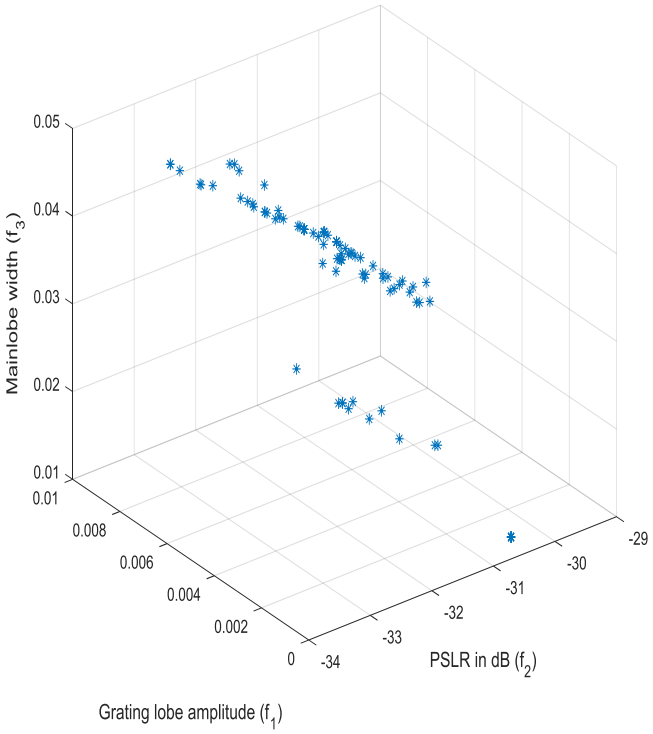

Figure 5: Pareto front determined by MOIDSA for $t_b\Delta f \in [2,10]$, $c \in [2,10]$ and N = 8.

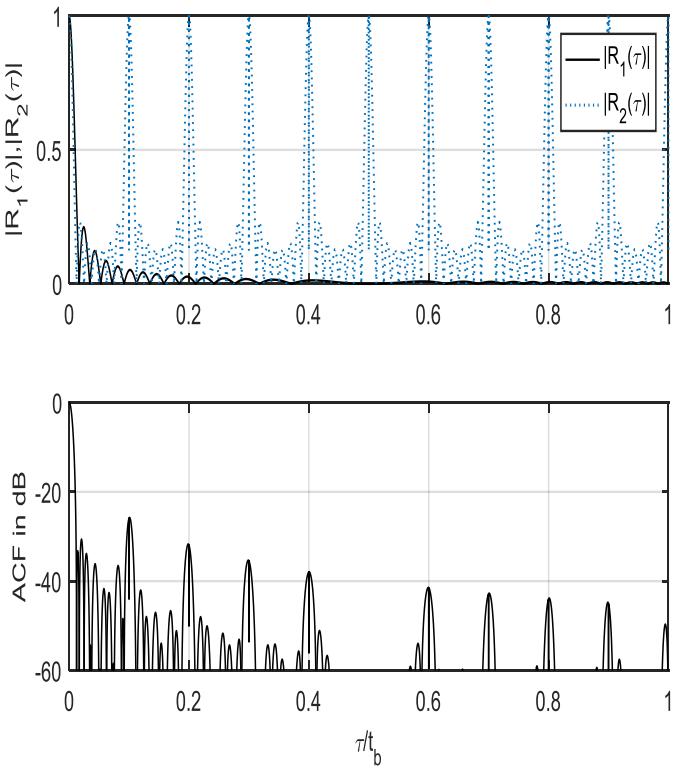

Figure 6: SFPT for $t_b\Delta f$ =10, c =5 and t_bB=60, N = 8. Top shows $|R_1(\tau)|$ and $|R_2(\tau)|$, bottom shows values of ACF (dB).

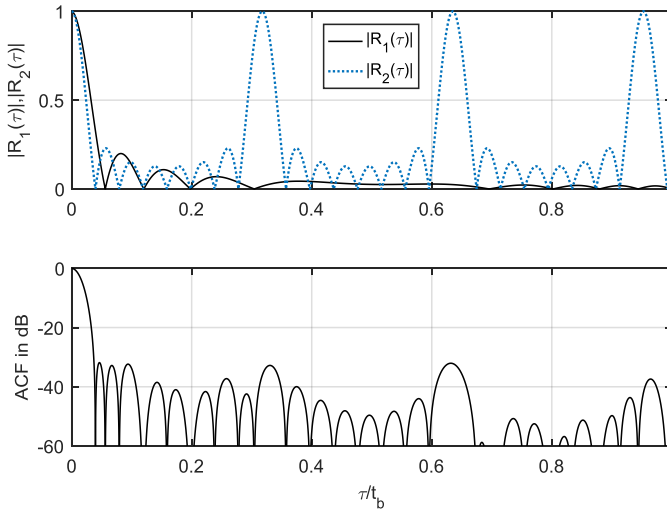

Figure 7: SFPT for $t_b\Delta f$ = 3.1490, c =5 and t_bB=18.894, N = 8. Top shows $|R_1(\tau)|$ and $|R_2(\tau)|$, bottom shows values of ACF (dB).

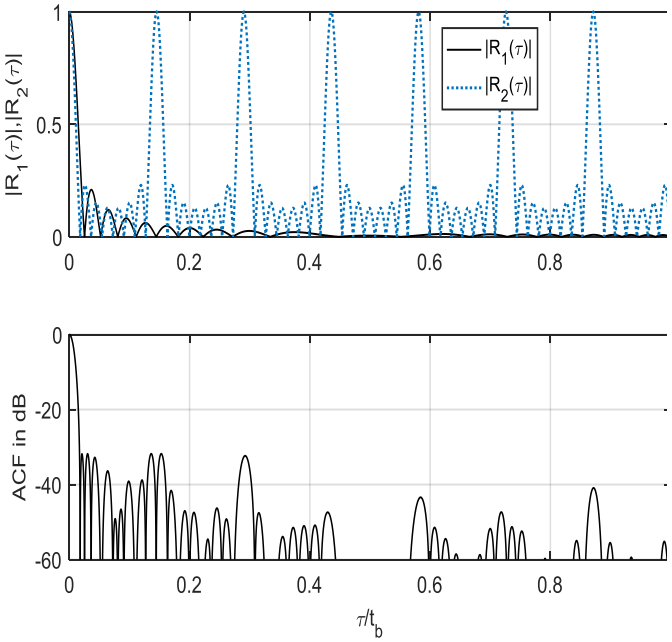

Figure 8: SFPT for $t_b\Delta f$ =6.8854, c =4.873 and t_bB = 40.438, N = 8. Top shows $|R_1(\tau)|$ and $|R_2(\tau)|$, bottom shows values of ACF (dB).

In the range $t_b\Delta f \in [2, 10]$, $c \in [2, 5]$ and N = 8 the PSLR is changed from -25.796 dB to -31.855dB shown in Figure 6, Figure 7 and Figure 8. The corresponding Pareto front is shown in Figure 9.

For $t_b\Delta f \in [5, 30]$, $c \in [2, 10]$ and N = 8, the PSLR is changed from -30.809 dB to -31.725 dB shown in Figure 10, Figure 11 and Figure 12 when $f_1 < 0.01$ and $f_3 < 0.045$ using MOIDSA. The corresponding Pareto front is shown in Figure 13. The values of grating lobes level, mainlobe width and PSLR are tabulated in table 1.

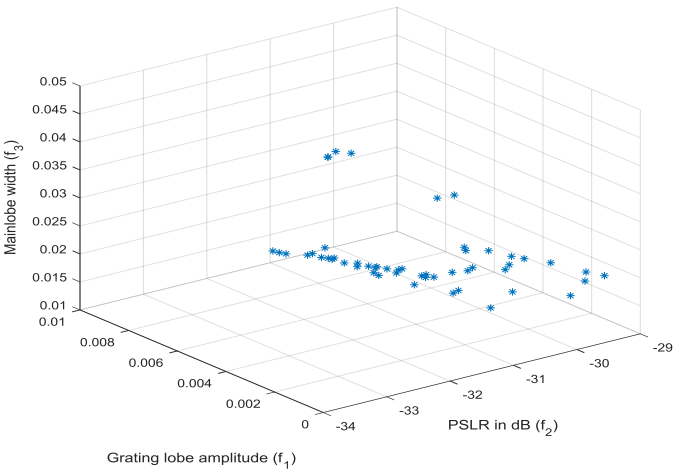

Figure 9: Pareto front obtained using MOIDSA for $t_b\Delta f \in [2, 10]$, $c \in [2, 5]$ and N = 8.

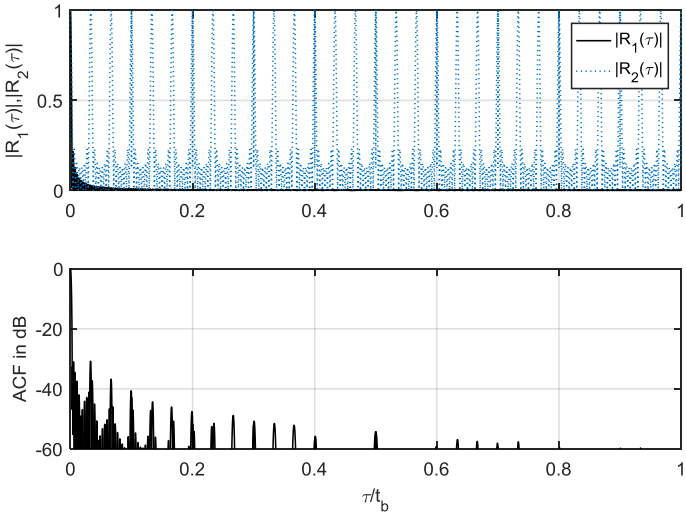

Figure 10: SFPT for $t_b\Delta f$ =30, c =10 and t_bB=330, N = 8. Top shows $|R_1(\tau)|$ and $|R_2(\tau)|$, bottom shows values of ACF (dB).

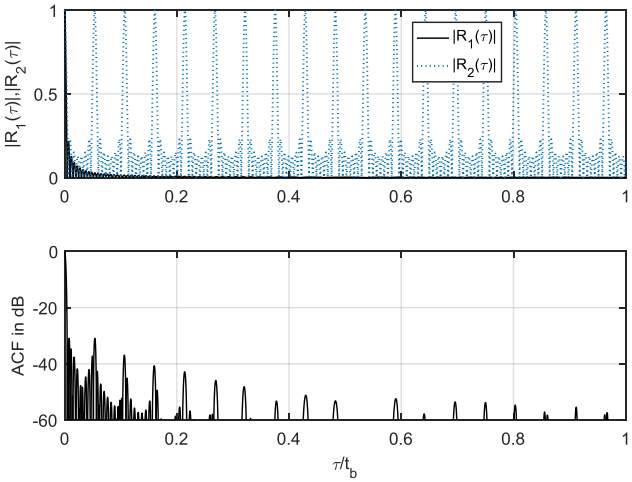

Figure 11: SFPT for $t_b\Delta f$ =18.6545, c =10 and t_bB=205.199, N = 8. Top shows $|R_1(\tau)|$ and $|R_2(\tau)|$, bottom shows values of ACF (dB).

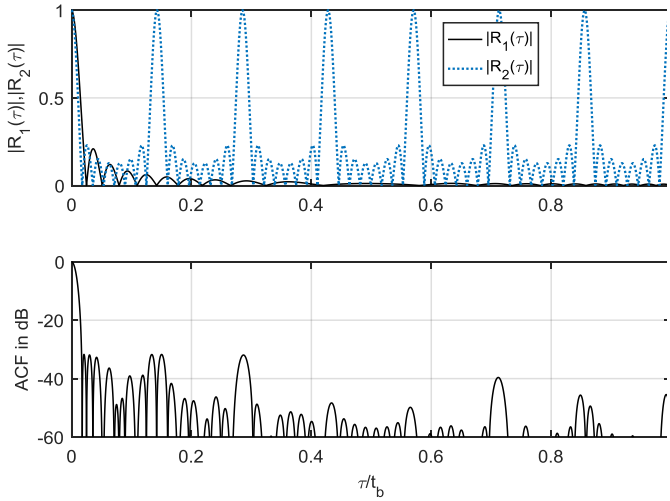

Figure 12: SFPT for $t_b\Delta f$ =7.0105, c =4.8556 and t_bB=41.051, N = 8. Top shows | $R_1(\tau)$ | and | $R_2(\tau)$ |, bottom shows values of ACF (dB).

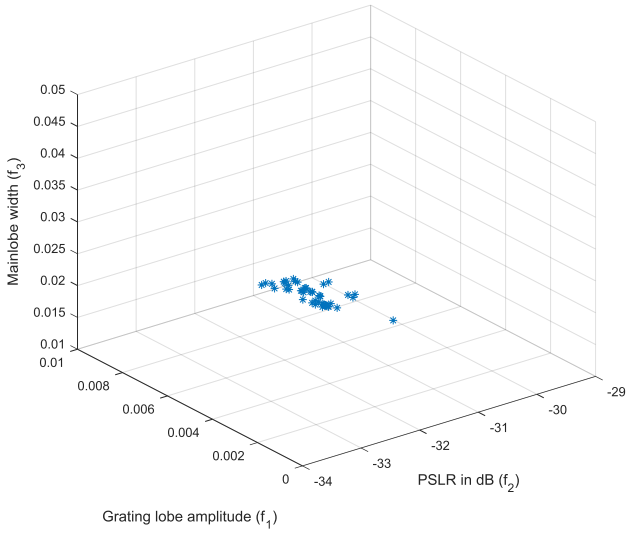

Figure 13: Pareto front obtained using MOIDSA for $t_b\Delta f \in [5, 30]$, $c \in [2, 10]$ and N = 8

Table 1: PSLR values obtained using MOIDSA.

Range		Grating lobe amplitude	Mainlobe width	PSLR (dB)
$t_b\Delta f$	c			
[2, 10]	[2, 10]	9.0909×10^{-11}	0.0125	-30.713
		0.0076	0.0417	-32.412
		0.0086	0.0414	-32.434
[2, 10]	[2, 5]	1.6667×10^{-10}	0.0125	-25.796
		0.0054	0.0397	-31.855
		0.0077	0.0182	-31.805
[5, 30]	[2, 10]	3.0303×10^{-11}	0.0042	-30.809
		0.0009	0.0067	-30.895
		0.007	0.0178	-31.725

According to the requirement of the application, this MOIDSA based SFPT can be used. If Peak sidelobe level is decreased, mainlobe width is increased that's why range resolution is decreased. When mainlobe width is decreased, Peak sidelobe level is increased, due to that small echoes cannot be detected. So this approach presents the compromise solution for grating lobes, PSLR and width of mainlobe. The narrow mainlobe width can be achieved with the cost of PSLR to obtain high range resolution. High PSLR can be achieved with the cost of range resolution to avoided false alarm. Hence depending upon the application requirement, the values of grating lobes and mainlobe width can be selected for high range resolution and low peak sidelobes.

The comparison of PSLR values for the SFPT parameters obtained from the MOIDSA and MOGOA [14] approaches are shown in Table 2 and Table 3.

Table 2: Comparison of PSLR values obtained by MOGOA and MOIDSA (f_1 versus f_2).

Range		PSLR in dB (MOGOA) [14]	PSLR in dB (MOIDSA)
$t_b\Delta f$	C		
[2, 10]	[2 , 10]	-32.329	-32.434
[2 ,10]	[2 ,5]	-31.860	-31.805
[5, 30]	[2 ,10]	-30.896	-31.725

Table 3: Comparison of PSLR values obtained by MOGOA and MOIDSA (f_2 versus f_3).

Range		PSLR in dB (MOGOA) [14]	PSLR in dB (MOIDSA)
$t_b\Delta f$	C		
[2, 10]	[2 , 10]	-32.291	-32.434
[2 ,10]	[2 ,5]	-31.851	-31.855
[5, 30]	[2 ,10]	-31.028	-31.725

Maximum PSLR is obtained as -32.434 dB when $t_b\Delta f \in [2, 10]$, $c \in [2, 10]$ by MOIDSA where as MOGOA is-32.329 dB for f_1 versus f_2 shown in table 2. For $t_b\Delta f \in [2, 10]$, $c \in [2, 10]$ the maximum PSLR obtained is -32.434 dB by MOIDSA and -32.291 dB using MOGOA for f_2 versus f_3 which is shown in table 3.

VI. CONCLUSIONS

In this endeavor, MOIDSA has been used to optimize parameters of SFPT to obtain low sidelobes, reduced mainlobe width and diminished grating lobes. For f_1 versus f_2, maximum PSLR of -32.434 dB is achived for $t_b\Delta f \in [2, 10]$, $c \in [2, 10]$.

Compared to MOGOA, -0.105 dB PSLR is improved in that range. When $t_b\Delta f \in [5, 30], c \in [2, 10]$, the PSLR is improved to -0.829 dB. For f_2 versus f_3, the improvement in PSLR for $t_b\Delta f \in [2, 10], c \in [2, 10]$; $t_b\Delta f \in [2, 10], c \in [2, 5]$ and $t_b\Delta f \in [5, 30], c \in [2, 10]$ are to be -0.143 dB, -0.004 dB and -0.697 dB respectively.

REFERENCES

1. Merrill I. Skolnik, Introduction to radar systems, McGraw Hill Book Company Inc., 1962.
2. Carpentier, Michel H., "Evolution of Pulse Compression in the Radar Field," Microwave Conference, 1979. 9th European , vol., no., pp.45-53, 17-20 Sept.1979.
3. Merrill I. Skolnik, "Introduction to Radar System.(3rd ed.)," NewYork: McGraw-Hill, 2002.
4. Fu, J.S. and Xin Wu, "Sidelobe suppression using adaptive filtering techniques", in Proc. CIE International Conference on Radar, pp.788-791, Oct. 2001.
5. R. L. Frank, "Polyphase Codes with Good Non periodic Correlation Properties", IEEE Trans. on Information Theory, vol. IT-9, pp. 43-45, Jan. 1963.
6. N. Levanon and E. Mozeson, Radar signals. John Wiley and Sons, Inc, 2004.
7. D. R. Wehner, High resolution Radar, Artech house, Boston, 1995.
8. D. E. Maron, "Non-periodic frequency-jumped burst waveforms," in Proceedings of the lEE International Radar Conference. London, pp. 484-488, Oct, 1987.
9. D. E. Maron, "Frequency-jumped burst waveforms with stretch processing," in Radar Conference, 1990., Record of the IEEE 1990 International. IEEE, pp. 274-279, 1990.
10. N. Levanon and E. Mozeson, "Nullifying ACF grating lobes in stepped frequency train of Ifm pulses," Aerospace and Electronic Systems, IEEE Transactions on, vol.39, no.2, pp. 694-703, 2003.
11. D. J. Rabideau, "Nonlinear synthetic wideband waveforms," in Radar Conference, 2002. Proceedings of the IEEE. pp. 212-219, 2002.
12. [A. K. Sahoo and G. Panda, "A multi-objective optimization approach to determine the parameters of stepped frequency pulse train," Aerospace science and technology vol.24, no.1, pp. 101-110, 2013.
13. K. Deb, A. Pratap, S. Agarwal, and T. Meyarivan, "A fast and elitist multi-objective genetic algorithm: Nsga-ii," Evolutionary Computation, IEEE Transactions on, vol. 6, no. 2, pp. 182-197, 2002.
14. K. R. Kumar and P. R. Kumar, "Performance Evaluation of Multi-Objective Grasshopper Optimization Algorithm to Reduce the Grating Lobes and Sidelobes," Jour of Adv Research in Dynamical & Control Systems, Vol. 10, 06-Special Issue, pp. 634 – 643, 2018.
15. Sarita Nanda, Milan Biswal, P.K. Dash, "Estimation of time varying signal parameters using an improved Adaline learning algorithm, AEU - International Journal of Electronics and Communications, Volume 68, Issue 2, Pages 115-129, 2014.
16. Li Li, Tian-shuang Qiu, De-rui Song, "Parameter estimation based on fractional power spectrum under alpha-stable distribution noise environment in wideband bistatic MIMO radar system, AEU - International Journal of Electronics and Communications, Volume 67, Issue 11, Pages 947-954, 2013.
17. Kaibo Cui, Weiwei Wu, Jingjian Huang, Xi Chen, Naichang Yuan, "DOA estimation of LFM signals based on STFT and multiple invariance ESPRIT, AEU - International Journal of Electronics and Communications, Volume 77, Pages 10-17, 2017.
18. N. Levanon, "Cross-correlation of long binary signals with longer mismatched filters," in IEE Proceedings - Radar, Sonar and Navigation, vol. 152, no. 6, pp. 377-382, 9 Dec. 2005.
19. Kurban T, Civicioglu P, Kurban R, Besdok E. Comparison of evolutionary and swarm based computational techniques for multilevel color image thresholding. Appl Soft Comput; 23:128–43, 2014.
20. Storn R, Price K. Differential evolution-a simple and efficient heuristic for global optimization over continuous spaces. J. Global Optim. 11(4):341–59, 1997.
21. Sowjanya Kotte, P. Rajesh Kumar, Satish Kumar Injeti, "An efficient approach for optimal multilevel thresholding selection for gray scale images based on improved differential search algorithm," Ain Shams Eng J (2016).
22. Injeti,S.K., "A Pareto optimal approach for allocation of distributed generators in radial distribution systems using improved differential search algorithm," J. Electr. Syst. Inform. Technol. (2017), http://dx.doi.org/10.1016/j.je